Comparison of Analytical Models for Predicting Electromagnetic Performance in Surface-Mounted Permanent Magnet Machines

L. J. Wu[1], Z. Q. Zhu[1], D. Staton[2], M. Popescu[2], and D. Hawkins[2]
[1]Department of Electronic and Electrical Engineering, University of Sheffield, Sheffield, UK.
Email: L.wu@sheffield.ac.uk, z.q.zhu@sheffield.ac.uk
[2]Motor Design Ltd, Lloyds Bank Chambers, 4 Scotland Street, Ellesmere, UK.
Email: dave.staton@motor-design.com,mircea.popescu @motor-design.com, dougie.hawkins@motor-design.com

***Abstract*-The paper compares four analytical models, viz. relative permeance (RP), complex permeance (CP), subdomain (SD) based on single slot/pole and exact SD, for predicting electromagnetic performance of surface-mounted permanent magnet brushless machines. The RP model is simple, takes less computational time for predicting electromagnetic torque although modification is often required to account for fringing effect. All analytical models predict the back-EMF and electromagnetic torque with high accuracy. The error in flux density associated with the CP model has less influence on electromagnetic torque but results in large error in cogging torque. As for the torque ripple excluding cogging torque, both SD models have similar waveforms and tend to underestimate, while RP and CP models tend to overestimate. Overall the SD models are most accurate for predicting the electromagnetic performance although much time consuming for computation.**

I. INTRODUCTION

In this paper, three recently developed analytical models, complex permeance model (CP) [1]-[2], subdomain model (SD) based on single slot/pole [3]-[5], and exact SD model [6]-[7], together with the relative permenace (RP) model [8]-[11], will be studied and compared for electromagnetic performance, such as back-EMF and electromagnetic torque, of surface-mounted permanent magnet (SPM) machines, while they are evaluated for cogging torque prediction in another paper [12]. The analytical models received much attention since they have advantage for the initial design and optimization of the machine. All analytical models to be studied are 2-D models which are much more accurate than 1-D model [13] in SPM machines due to large effective air-gap length.

Both RP and CP models are derived from the conformal mapping. The RP model used a simplified relative permeance and only one point in the waveform needs to be calculated by the conformal mapping [10], while every point in the complex permeance is numerically calculated in the CP model [1]-[2]. The imaginary component of the CP makes it possible to consider the influence between radial and tangential components of flux density due to slotting effect. The excellent accuracy of the CP model for air-gap flux density and back-EMF waveform was demonstrated in [1]. A combined CP model was presented in [14] and is much faster. Partially [3]-[4] and completely [5] in polar coordinates, an SD model was developed to account for slotting effect, which solved the field governing function in each simple SD and obtained the final solution by applying boundary conditions between SDs. However, this SD model is only for machines having radially magnetized magnets and was derived from a simplified model which has one slot per pole. This simplification approximates the mutual influence between slots. The model was extended in [7] for parallel magnetized magnets, but the model was only for integer-slot machines. Reference [7] also tried to account for the mutual influence between slots but with serious mistakes. An exact model was presented in [6] for SPM machines of any pole and slot combinations accounting for the influence of interaction between slots, radial/parallel magnetization, internal/external rotor topologies, relative recoil permeability of magnets, and odd/even periodic boundary conditions.

In this paper, the comparison between above-mentioned four analytical models, viz. relative permeance (RP), complex permenace (CP), subdomain (SD) model based on single slot/pole and exact SD model, will be carried out on a 4-pole/24-slot machine having internal rotor configuration. The FE will be performed using python scripting in FLUX 2D to provide the reference for comparison.

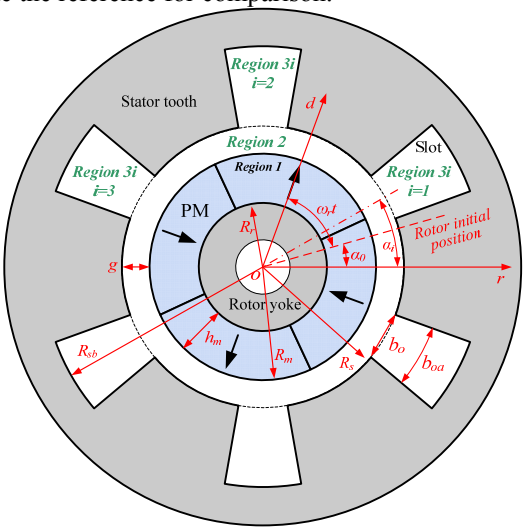

Fig. 1. Symbols and cross-section of SPM machine.

978-1-4244-8218-4/10/$26.00 ©2010 Crown

II. ANALYTICAL MODELS FOR ELECTROMAGNETIC PERFORMANCE

A. Relative Permeance Model

Some assumptions such as infinite permeable iron, linear magnet property, and negligible end-effect, are made in all analytical models, while the tooth-tip is simplified to be straight as shown in Fig. 1.

The air-gap flux density of SPM machine on open-circuit neglecting the slots can be expressed as:

$$B_{mr}(r,\alpha)=\sum_{n=1,3,\cdots}^{\infty} B_{rn}\sin\left(np\alpha-np\omega_r t-np\alpha_0+\pi/2\right) \quad (1)$$

for radial component, and

$$B_{m\alpha}(r,\alpha)=\sum_{n=1,3,\cdots}^{\infty} B_{\alpha n}\sin\left(np\alpha-np\omega_r t-np\alpha_0\right) \quad (2)$$

for circumferential component, where p is the number of pole pairs, r and α are the radius and circumferential position, α_0 is the rotor initial position, ω_r is the mechanical speed, and B_{rn} and B_{an} are magnitudes of the n^{th} order harmonics of radial and tangential air-gap flux density and their expressions can be found in [8-9].

The radial component of PM field on the stator bore accounting for slots can be expressed by [10]:

$$B_r\big|_{r=R_s}=B_{mr}\big|_{r=R_s}\cdot\lambda \quad (3)$$

where R_s is the radius of the stator bore. The relative air-gap permeance λ was given as:

$$\lambda=K_f\begin{cases}1-\beta(r)-\beta(r)\cos\dfrac{\pi}{0.8b_{oa}}\alpha & 0\le\alpha\le 0.8b_{oa}\\ 1 & 0.8b_{oa}\le\alpha\le\tau_t/2\end{cases} \quad (4)$$

where $b_{oa}=b_o/R_s$, b_o is the slot opening width, τ_t is the slot pitch angle, β is obtained from the conformal mapping and was given in [10], and K_f is the fringing compensation coefficient for fringing effect.

This RP has a predetermined waveform shape with one point in the middle of the slot opening determined by the conformal mapping. It takes the fringing effect (flux focusing) into account by using the compensation coefficient K_f. If K_f is neglected, the predicted back-EMF and electromagnetic torque tends to be lower than the real value depending on the slot opening width. By way of example, the RP with/without considering K_f, and RP without fringing, together with the accurate relative permeance, of which every point is predicted by the conformal mapping, of the 4-pole/24-slot machine on the stator bore are shown in Fig. 2. As seen in the figure, the point of the RP without considering K_f in the middle of slot opening is accurate. The fringing flux near tooth tips is considered, but underestimated. It is increased by considering K_f to make the average value the same as the accurate RP.

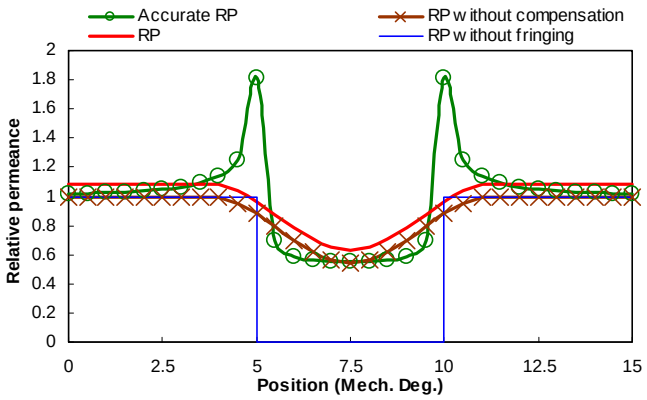

Fig. 2. Relative permeance waveforms of 4-pole/24-slot machine, slot opening spans between 5-10 Mech. Deg., $r=R_s$.

Compared with the RP without fringing effect as shown in Fig. 2, the fringing coefficient of the RP can be expressed as:

$$K_{f1}=\frac{\phi_{RP}}{\phi_o}=\frac{\tau_t-1.6\beta b_{oa}}{\tau_t-b_{oa}}K_f \quad (5)$$

where ϕ_{RP} is the main flux predicted by the RP and ϕ_o is the main flux neglecting fringing.

With respect to the RP without fringing effect, the fringing coefficient of the accurate RP (Fig. 2) can be predicted by the conformal mapping [15] and expressed as:

$$K_{f2}=\frac{\phi_a}{\phi_o}=\frac{2g'}{\tau_t R_s-b_o}\frac{\nu_2}{\pi} \quad (6)$$

where ϕ_a is the main flux predicted by the accurate RP and ν_2 satisfies:

$$\begin{cases} t=2\left(g'/b_o\right)^2\left(\cosh\nu_2-1\right)\\ \dfrac{1}{2}\left(\tau_t R_s-b_o\right)=-\dfrac{b_o}{\pi}\arctan\left(\dfrac{2g'}{b_o}\sqrt{\dfrac{t-1}{t+\left(2g'/b_o\right)^2}}\right)\\ \qquad\qquad +\dfrac{g'}{\pi}\ln\left(\dfrac{\sqrt{t+\left(2g'/b_o\right)^2}+\sqrt{t-1}}{\sqrt{t+\left(2g'/b_o\right)^2}-\sqrt{t-1}}\right)\end{cases} \quad (7)$$

where $g'=g+h_m/\mu_r$, g is the air-gap length, h_m is the thickness of magnets, and μ_r is the relative permeability of magnets.

Thus, in order to accurately account for the fringing flux, i.e. $\phi_{RP}=\phi_a$, K_{f1} should be equal to K_{f2}, then the fringing compensation coefficient can be obtained as:

$$K_f=\frac{2g'}{\tau_t R_s-b_o}\frac{\nu_2}{\pi}\frac{\tau_t-b_{oa}}{\tau_t-1.6\beta b_{oa}} \quad (8)$$

The RP can also be expressed as Fourier series:

$$\lambda=\lambda_0+\sum_{b=1,2,3,\ldots}\lambda_{rc}\cos\left(bN_s\alpha-b\alpha_{s0}\right) \quad (9)$$

where N_s is the slot number, λ_0 and λ_{rc} are the average value and harmonic magnitude of the air-gap RP, respectively, and

$$\alpha_{s0}=\begin{cases}0 & \text{coil spans odd number of slots}\\ \pi/N_s & \text{coil spans even number of slots}\end{cases} \quad (10)$$

By approximating the coil as a current sheet over the slot opening, the phase flux-linkage can be predicted based on the radial flux density distribution along the stator bore [1, 11]:

$$\psi_j = l_a R_s N \sum_{n=1,3,5...} K_{dn} \left\{ \frac{2B_{rn}\lambda_0}{np} K_p\left(np,\alpha_y\right) K_{so}\left(np,b_{oa}\right) + \sum_b \left[\frac{B_{rn}\lambda_{rc}}{np+bN_s} K_p\left(np+bN_s,\alpha_y\right) K_{so}\left(np+bN_s,b_{oa}\right) + \frac{B_{rn}\lambda_{rc}}{np-bN_s} K_p\left(np-bN_s,\alpha_y\right) K_{so}\left(np-bN_s,b_{oa}\right) \right] A_b \right\} \cdot \cos\left(np\omega_r t - n\alpha_j\right) \quad (11)$$

where l_a is the active length, N is the number of phase series turns, j stands for phase A, B, and C, respectively, α_j is equal to 0 for phase A, 2π/3 for phase B, and 4π/3 for phase C, α_y is the coil pitch, i.e. coil span, in mech. radian,

$$A_b = \begin{cases} 1 & \text{coil spans odd number of slots} \\ \cos b\pi & \text{coil spans even number of slots} \end{cases} \quad (12)$$

$$N_{s0} = \frac{N_s}{3GCD\left(2p,N_s\right)} \quad (13)$$

when N_{s0} is odd:

$$K_{dn} = \frac{\sin\left(n\frac{\pi}{6}\right)}{N_{s0}\sin\left(n\frac{\pi}{6N_{s0}}\right)} \quad (14)$$

when N_{s0} is even:

$$K_{dn} = \frac{2\sin\left(n\frac{\pi}{6}\right)}{N_{s0}\sin\left(n\frac{\pi}{3N_{s0}}\right)} \quad (15)$$

$$K_p\left(C_I,\alpha_y\right) = \sin\left(C_I\alpha_y/2\right) \quad (16)$$

$$K_{so}\left(C_I,b_{oa}\right) = \frac{\sin\left(C_I b_{oa}/2\right)}{C_I b_{oa}/2} \quad (17)$$

where C_I is an integer number.

Thus, the back-EMF is expressed by:

$$e_j = l_a R_s N \sum_{n=1,3,5...} K_{dn} \left\{ 2B_{rn}\lambda_0 K_p\left(np,\alpha_y\right) K_{so}\left(np,b_{oa}\right) + \sum_b \left[\frac{npB_{rn}\lambda_{rc}}{np+bN_s} K_p\left(np+bN_s,\alpha_y\right) K_{so}\left(np+bN_s,b_{oa}\right) + \frac{npB_{rn}\lambda_{rc}}{np-bN_s} K_p\left(np-bN_s,\alpha_y\right) K_{so}\left(np-bN_s,b_{oa}\right) \right] A_b \right\} \cdot \sin\left(np\omega_r t - n\alpha_j\right) \quad (18)$$

The electromagnetic torque can be calculated by:

$$T_{em} = \left(e_a i_a + e_b i_b + e_c i_c\right)/\omega_r \quad (19)$$

B. Complex Permeance Model

By using the CP model, the radial and circumferential components of PM air-gap flux densities accounting for slots can be expressed by [1]:

$$B_r = B_{mr}\lambda_{real} + B_{m\alpha}\lambda_{imag} \quad (20)$$

$$B_\alpha = B_{m\alpha}\lambda_{real} - B_{mr}\lambda_{imag} \quad (21)$$

where λ_{real} and λ_{imag} are the real and imaginary components of the relative CP function introduced for slotting effect, respectively, and could be found in [1-2].

The radial air-gap flux density on the stator bore accounting for slots can be given by:

$$B_r\Big|_{r=R_s^-} = B_{mr}\Big|_{r=R_s^-}\lambda_{real} \quad (22)$$

where R_s^- is a radius not exactly on but close to the stator bore to avoid the singularity.

Comparing (22) with (3), the CP model is very similar to the RP model. Thus, the prediction of back-EMF and electromagnetic torque by the CP model is also similar to (9)-(19). One difference is that the RP is a simplified function with a predetermined waveform shape and only one point to be predicted by conformal mapping, while every point of the CP is calculated by conformal mapping as mentioned earlier. Thus, the CP function is more accurate and the fringing compensation coefficient K_f employed in the RP model is not required in the CP model. Another difference is that the tangential flux density is also given in the CP model and hence the cogging torque can be predicted by applying the Maxwell stress tensor in the air-gap:

$$T_c = \left(l_a r^2/\mu_0\right)\int_0^{2\pi} B_r B_\alpha d\alpha \quad (23)$$

However, it will be shown that the CP model still has some error due to neglecting the deformations of magnets and path to predict flux density in the conformal mapping, Fig. 3.

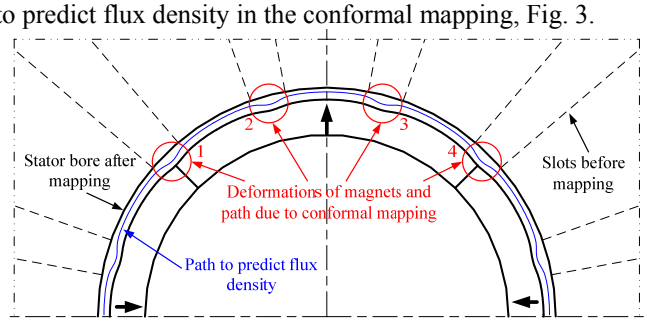

Fig. 3. Deformation of magnets and path in the middle of air-gap due to conformal mapping. Dashed/solid line: geometry before/after mapping.

C. Subdomain Model

In the subdomain model, the air-gap flux density accounting for slots is expressed by [6]:

$$B_{rSD} = B_{mr} - \sum_k g_{Br} A_{stator} \cos k\alpha - \sum_k g_{Br} B_{stator} \sin k\alpha \quad (24)$$

$$B_{\alpha SD} = B_{pm\alpha} - \sum_k g_{B\alpha} B_{stator} \cos k\alpha + \sum_k g_{B\alpha} A_{stator} \sin k\alpha \quad (25)$$

where g_{Br} and $g_{B\alpha}$ are the contribution factors of the scalar potential distribution along the stator bore to the air-gap flux densities, which are given in [6], and A_{stator} and B_{stator} are cosine and sine components of the scalar potential distribution harmonics along the stator bore, respectively:

$$A_{stator}\left(k\right) = \sum_{i=1}^{N_s}\sum_{m=1}^{m_{\max}} C_{ei}\left(m\right)\eta_{si}\left(m,k\right) \quad (26)$$

$$B_{stator}(k)=\sum_{i=1}^{N_s}\sum_{m=1}^{m_{\max}}\sum_{m}C_{ei}(m)\xi_{si}(m,k) \tag{27}$$

where $C_{ei}(m)$ is the m^{th} order harmonic of the scalar potential distribution along the i^{th} slot opening, η_{si} and ξ_{si} can be found in [6], and $\mathbf{C_{ei}}=[C_{ei}(1), C_{ei}(2), ..., C_{ei}(m_{\max})]^T$ can be calculated by:

$$\mathbf{C_{ei}}=\mathbf{Z_{si}}^{-1}\mathbf{Y_{si}} \tag{28}$$

$$\mathbf{Z_{si}}=\mathbf{W_e}+\hat{\mathbf{P}}_{si}\hat{\boldsymbol{\eta}}_{si}{}^{T}+\hat{\mathbf{Q}}_{si}\hat{\boldsymbol{\xi}}_{si}{}^{T} \tag{29}$$

where the detail of $\mathbf{Z_{si}}$, a $M\times M$ matrix, is given in [6]. According to (28)-(29), the mutual influence between slots is neglected and the slots are accounted for one by one. The original model [3-5] is a model having one slot per pole as shown in Fig. 4 in the calculation of the scalar potential distribution along each slot opening. Thus, this SD model [3-5] is named as the SD model based on single slot/pole.

In the exact SD model, the scalar potential distribution along all slots $\mathbf{C_{et}}=[\mathbf{C_{e1}}, \mathbf{C_{e2}}, ..., \mathbf{C_{eNs}}]^T$ is calculated together by:

$$\mathbf{C_{et}}=\mathbf{Z_{st}}^{-1}\mathbf{Y_{st}} \tag{30}$$

$$\mathbf{Z_{st}}=\mathbf{W_{et}}+\mathbf{P_{st}}\boldsymbol{\eta}_{st}{}^{T}+\mathbf{Q_{st}}\boldsymbol{\xi}_{st}{}^{T} \tag{31}$$

where the detail of $\mathbf{Z_{st}}$, a $MN_s\times MN_s$ matrix, is given in [6].

Based on the foregoing analysis, it can be seen that the computation of A_{stator} and B_{stator} requires to solve N_s sets of M^2 equation sets in the SD model based on single slot/pole or a $N_s^2M^2$ equation set in the exact SD for each rotor position. It is very time-consuming since such calculation is needed for each rotor position.

By approximating the coil as a current sheet over the slot opening, the phase flux-linkage can be predicted by the integral of the radial flux density distribution along the stator bore:

$$\psi_j=2l_aR_sN\sum_k\frac{1}{k}K_pK_{so}\left(B_{rs}K_{dsj}+B_{rc}K_{dcj}\right)\quad j=A,B,C \tag{32}$$

where B_{rs} and B_{rc} are sine and cosine harmonics of radial flux density at the stator bore, respectively, K_p is the pitch factor, K_{so} is the slot opening factor, K_{dsj} and K_{dcj} are the distribution factors of phase j for sine and cosine flux density harmonics, respectively. These factors can be given by:

$$K_p=\sin k\frac{\alpha_y}{2} \tag{33}$$

$$K_{so}=\frac{\sin\left(kb_{oa}/2\right)}{kb_{oa}/2} \tag{34}$$

$$K_{dsj}=\frac{1}{n_c}\sum_{s=1}^{n_c}C_{ds}\sin k\alpha_{cs} \tag{35}$$

$$K_{dcj}=\frac{1}{n_c}\sum_{s=1}^{n_c}C_{ds}\cos k\alpha_{cs} \tag{36}$$

where n_c is the number of coils per phase, α_{cs} is the position of the s^{th} coil of phase j, C_{ds} is equal to 1 or -1 for connection with positive or negative polarity for the s^{th} coil of phase j.

The back-EMF can be calculated by:

$$e_j=\omega_r\frac{d\psi_j}{d\alpha}\quad j=A,B,C \tag{37}$$

The expressions of electromagnetic and cogging torque are the same as (19) and (23), respectively.

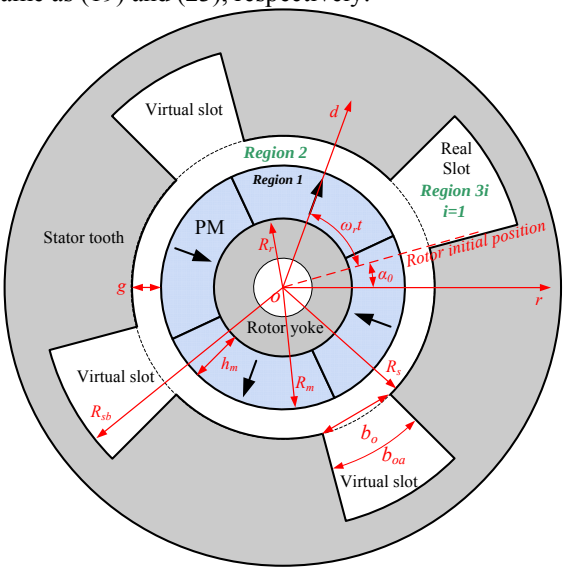

Fig. 4. Approximate one slot/pole model for one slot.

III. Comparison of FE and Analytically Predicted Results

The comparison is carried out on a 4-pole/24-slot machine whose parameters are shown in Table I.

TABLE I
MAJOR MACHINE PARAMETER (DEFAULT UNIT: MM)

Rated speed (rpm)	400	Tooth tip edge	1
Stator outer diameter	100	Stator inner diameter	48
Air-gap length	1	Rotor outer diameter	46
Slot opening	2	Stator yoke height	8.1
Axial length	50	Tooth body width	3.1
Magnet thickness	3	Winding turns / phase	104
B_r (T)/μ_r	1.2/1.05	Coil pitch (slots)	5
Magnetization	Parallel	Rated current (A)	10

A. Air-gap Flux Density

The analytically and FE predicted airgap flux density distributions are compared in Fig. 5, where only a quarter cycle is shown for clarity since the machine has integer-slot winding. It shows that the RP model without compensation of fringing effect predicts smaller results since the fringing effect is serious for the machine having a large slot opening width. Although the flux density distribution predicted by the RP model still has some difference from FE prediction near tooth-tips, the fundamental flux density is very close to that obtained by FE and hence the predicted back-EMF and electromagnetic is expected to be very accurate. The subdomain models show the most accurate results, while the flux density predicted by the CP model generally has high accuracy but has some error in area where the slot opening facing the rotor pole transition due to neglected deformation (around 0 deg. in Fig. 5(b)) as mentioned earlier. The error

can result in low accuracy of predicted cogging torque as shown in [12] but will be shown to have less influence on the back-EMF and electromagnetic torque later.

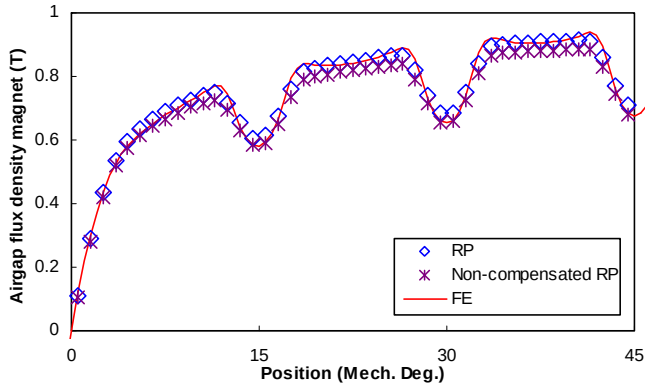

(a) RP

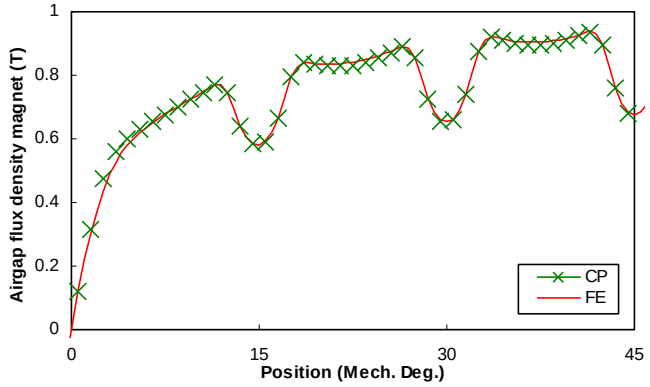

(b) CP

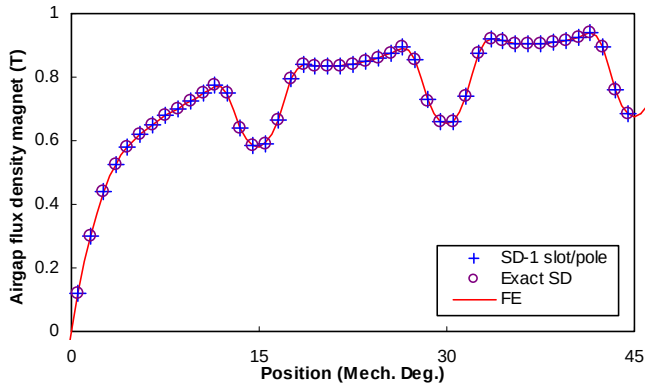

(c) SD

Fig. 5. Analytically and FE predicted radial airgap flux density distributions.

B. Back-EMF, Electromagnetic and Cogging Torque

Since the RF model without compensation predicts smaller flux density, the predicted back-EMF and electromagnetic torque are very smaller than FE prediction as seen in Fig. 6. The RP model predicts similar waveforms to FE.

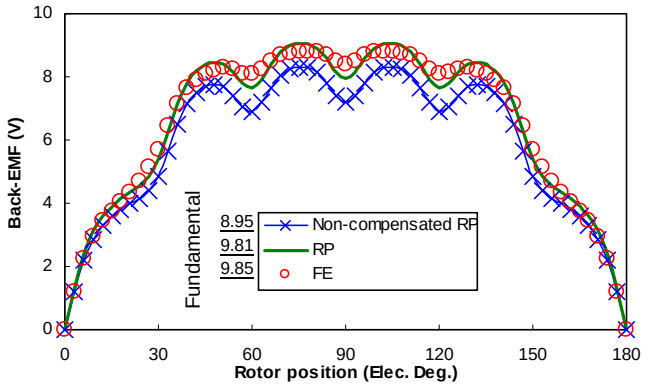

(a) Back-EMF

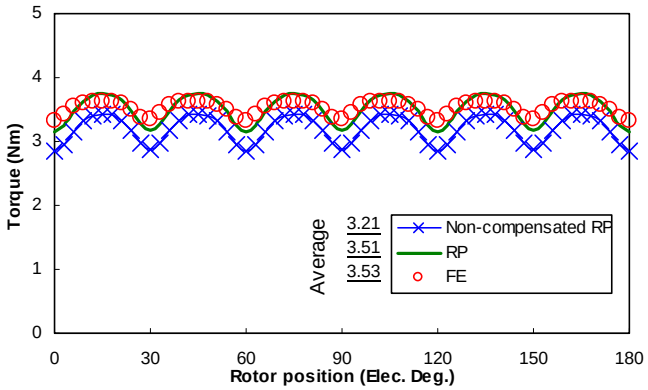

(b) Electromagnetic torque

Fig. 6. Comparison between back-EMF and torque waveforms predicted by RP model with/without compensation.

As seen in Fig. 7, all analytical models predict similar fundamental back-EMF and average electromagnetic torque to FE, but shows different torque ripples. For the fundamental back-EMF and average torque, the SD models exhibits the highest accuracy. The CP model also shows high accuracy, since the low accuracy part of the predicted flux density predicted has less influence on the fundamental back-EMF and average torque, but large influence on the cogging torque as shown in [12]. Although the flux density distribution predicted by the RP model has some difference from FE prediction, it also predict high accuracy of fundamental back-EMF and average torque since the compensation is for achieving the same main PM flux. As for the torque ripple, the subdomain models have similar waveforms and tend to underestimate due to approximating the coil as a current sheet over the slot opening, while RP and CP models tend to overestimate for this machine. Considering the computational time and complexity, the RP model is still a good choice for predicting electromagnetic performance of SPM machines.

As for cogging torque, it is much more difficult to predict the cogging torque accurately by using RP model although a modified analytical RP model may be employed [16]. Both SD models have excellent accuracy, while the CP shows a large error in magnitude, 74% with respect to the FE prediction. The low accuracy of the CP model is also observed in [12].

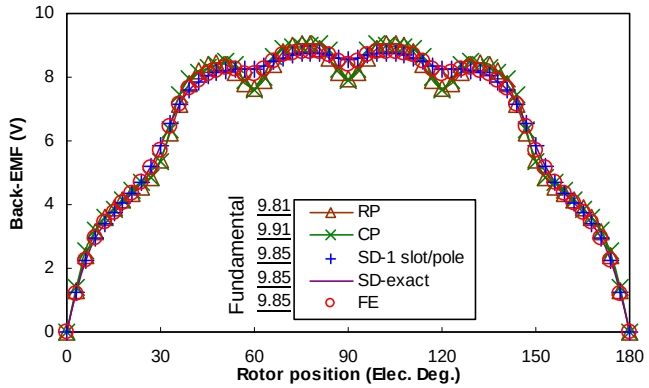

(a) Back-EMF

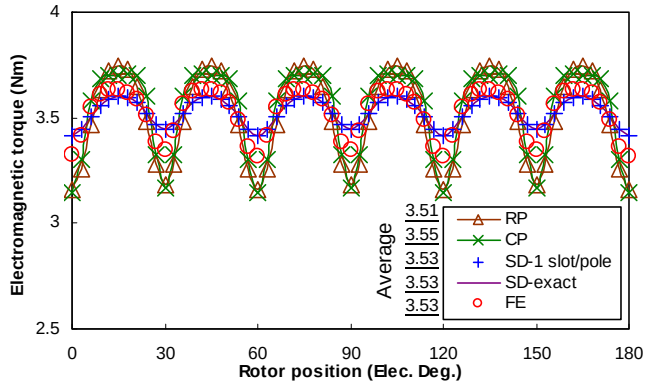

(b) Electromagnetic torque

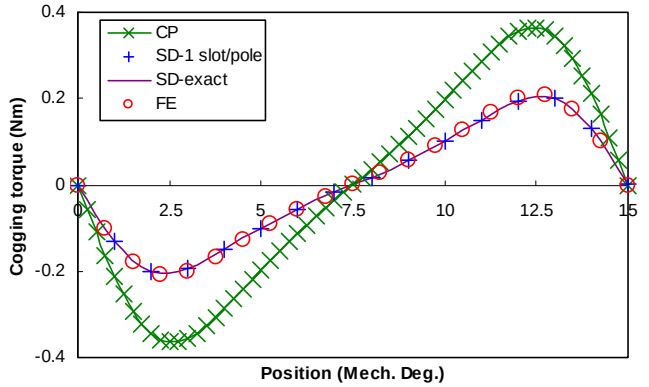

(c) Cogging torque

Fig. 7. Analytically and FE predicted back-EMF and torque waveforms.

IV. CONCLUSIONS

The paper has compared four analytical models, viz. relative permeance, complex permeance, subdomain based on single slot/pole and exact subdomain, for predicting electromagnetic performance of surface-mounted permanent magnet brushless machines. The RP model is simple and takes less computational time although modification is often required to account for fringing effect. The investigation shows that all analytical models predict the back-EMF and electromagnetic torque with high accuracy. The error in flux density associated with the CP model has less influence on electromagnetic performance but results in large error in the cogging torque. The SD models exhibit the highest accuracy for the fundamental back-EMF, average torque, and cogging torque. As for the torque ripple, the SD models have similar waveforms and tend to underestimate, while RP and CP models tend to overestimate. Overall the SD models are most accurate for predicting the electromagnetic performance although much time consuming for computation.

ACKNOWLEDGMENT

This work is financially supported by the Engineering and Physics Science Research Council, UK, Ref. EP/F016506/1., and Motor Design Ltd under the Motor-CAD/FLUX Partnership Scheme.

REFERENCES

[1] D. Zarko, D. Ban, and T. A. Lipo, "Analytical calculation of magnetic field distribution in the slotted air gap of a surface permanent-magnet motor using complex relative air-gap permeance," *IEEE Trans. Magnetics*, vol. 42, no. 7, pp. 1828-1837, 2006.

[2] D. Zarko, D. Ban, and T. A. Lipo, "Analytical solution for cogging torque in surface permanent-magnet motors using conformal mapping," *IEEE Trans. Magnetics*, vol. 44, no. 1, pp. 52-65, 2008.

[3] Z. J. Liu and J. T. Li, "Analytical solution of air-gap field in PM motors taking into account the effect of pole transition over slots," *IEEE Trans. Magnetics*, vol. 43, no. 10, pp.3872-3883, 2007.

[4] Z. J. Liu and J. T. Li, "Accurate prediction of magnetic field and magnetic forces in PM motors using an analytical solution," *IEEE Trans. Energy conversion*, vol. 23, no. 3, pp. 717-726, 2008.

[5] Z. J. Liu, J. T. Li, and Q. Jiang, "An improved analytical solution for predicting magnetic forces in permanent magnet motors," *Journal of Applied Physics*, vol. 103, no. 7, 2008.

[6] Z. Q. Zhu, L. J. Wu, and Z. P. Xia, "An accurate sub-domain model for magnetic field computation in slotted surface-mounted permanent magnet machines," *IEEE Trans. Magnetics*, vol. 46, no. 4, pp. 1100-1115.

[7] F. Dubas and C. Espanet, "Analytical solution of the magnetic field in permanent-magnet motors taking into account slotting effect: no-load vector potential and flux density calculation," *IEEE Trans. Magnetics*, vol. 45, no. 5, pp. 2097-2109, 2009.

[8] Z. Q. Zhu, D. Howe, E. Bolte, and B. Ackermann, "Instantaneous magnetic field distribution in brushless PM dc motors. Part I: Open-circuit field," *IEEE Trans. Magnetics*, vol.29, no.1, pp.124-135, 1993

[9] Z. Q. Zhu, D. Howe, and C. C. Chan, "Improved analytical model for predicting the magnetic field distribution in brushless PM machines," *IEEE Trans. Magnetics*, vol. 38, no. 1, pp.229-238, 2002.

[10] Z. Q. Zhu and D. Howe, "Instantaneous magnetic field distribution in brushless permanent magnet dc motors. Part III: Effect of stator slotting," *IEEE Trans. Magnetics*, vol. 29, no. 1, pp. 143-151, 1993.

[11] Z. Q. Zhu and D. Howe, "Instantaneous magnetic field distribution in permanent magnet brushless dc motors. Part IV: Magnetic field on load," *IEEE Trans. Magnetics*, vol. 29, no. 1, pp. 152-158, 1993.

[12] L. J. Wu, Z. Q. Zhu, D. Staton, M. Popescu, and D. Hawkins, "Comparison of analytical models for predicting cogging torque in surface-mounted PM machines," submitted to *ICEM 2010*.

[13] T. J. E. Miller, *Brushless permanent-magnet and reluctance motor drives*: Oxford Science Publications, 1993.

[14] L. J. Wu and Z. Q. Zhu, "Combined complex permeance and sub-domain model for analytical predicting electromagnetic performance of surface-mounted PM machines," presented at 5th Int. Conf. Power Electronics, Machines and Drives, Brighton, UK, 2010.

[15] L. V. Bewley, *Two-dimensional fields in electrical engineering*, The Macmillan Company, New York, 1948.

[16] Z. Q. Zhu and D. Howe, "Analytical prediction of the cogging torque in radial-field permanent magnet brushless motors," *IEEE Trans. Magnetics*, vol. 28, no. 2, pp. 1371-1374, 1992.